ELSEVIER

Biochimica et Biophysica Acta 1235 (1995) 395–405

BBA Biochimica et Biophysica Acta

Phospholipase A_2 domain formation in hydrolyzed asymmetric phospholipid monolayers at the air/water interface

Kevin M. Maloney [a], Michel Grandbois [b], David W. Grainger [c,*], Christian Salesse [b], Karen A. Lewis [d], Mary F. Roberts [d]

[a] *Department of Chemistry, Biochemistry and Molecular Biology, Oregon Graduate Institute of Science and Technology, Portland, OR, USA*
[b] *Centre de Recherche en Photobiophysique, Université du Québec à Trois-Rivières, C.P. 500, Trois-Rivières, Qué., G9A 5H7, Canada*
[c] *Department of Chemistry, Colorado State University, Fort Collins, CO 80523, USA*
[d] *Department of Chemistry, Boston College, Chestnut Hill, MA, USA*

Received 8 November 1994; accepted 29 November 1994

Abstract

Phospholipase A_2 (PLA_2) catalyzed hydrolysis of asymmetric 1-caproyl-2-palmitoyl-phosphatidylcholine (6,16-PC) and 1-palmitoyl-2-caproyl-phosphatidylcholine (16,6-PC) lipid monolayers at the air/water interface was investigated. Surface pressure isotherms, surface potential and fluorescence microscopy at the air/water interface were used to characterize the asymmetric monolayer systems. Cobra (*N. naja naja*) and bee venom PLA_2 exhibit hydrolytic activity towards 6,16-PC and 16,6-PC monolayers at all surface pressures up to monolayer collapse (37 mN m^{-1}). Pancreatic PLA_2 hydrolytic activity, however, was observed to be blocked at a lateral surface pressure of approx. 18 mN m^{-1} for both 6,16-PC and 16,6-PC monolayers. For 6,16-PC monolayers, fluorescence microscopy revealed that monolayer hydrolysis by PLA_2 from cobra, bee, and bovine pancreatic sources all produced monolayer microstructuring. Fluorescence microscopy also showed that PLA_2 is bound to these monolayer microstructures. Very little PLA_2-induced microstructuring was observed to occur in 16,6-PC monolayer systems where caproic acid (C6) hydrolysis products were readily solubilized in the aqueous monolayer subphase. Surface potential measurements for 16,6-PC monolayer hydrolysis indicate dissolution of caproic acid reaction products into the monolayer subphase. Monolayer molecular area as a function of 6,16-PC monolayer hydrolysis time indicates the presence of monolayer-resident palmitic acid reaction products. With bovine serum albumin present in the monolayer subphase, PLA_2 domain formation was observed only in hydrolyzed 6,16-PC monolayers. These results are consistent with laterally phase separated monolayer regions containing phospholipid and insoluble fatty acid reaction products from PLA_2 monolayer hydrolysis electrostatically driving PLA_2 adsorption to and enzyme domain formation at the heterogeneous, hydrolyzed lipid monolayer interface.

Keywords: Phospholipase A_2; Domain formation; Fluorescence microscopy; Surface potential; Monolayer; Air/water interface; Asymmetric lipid; Fatty acid

1. Introduction

Phospholipase A_2 (PLA_2, EC 3.1.1.4) is an interfacially activated enzyme that catalyzes stereospecific hydrolysis of *sn*-2 acyl ester linkages of *sn*-3-glycerophospholipids [1], producing fatty acid and lyso-lipid products. It is well recognized that PLA_2 action towards lipid membrane interfaces (vesicles, multilamellar dispersions, and monolayers) is much higher than toward isotropically dispersed phospholipids [2]. Previously, our studies with coworkers have shown that PLA_2-hydrolyzed phospholipid monolayers at the air/water interface exhibit two-dimensional (2-D) enzyme domains in the monolayer plane [3,4]. A scheme describing interfacial PLA_2 domain formation has been proposed [3,4] where PLA_2 adsorbs electrostatically to phase separated regions enriched in fatty acid reaction products released by PLA_2 in the monolayer membrane.

Using fluorescence microscopy at the air/water interface, we have recently investigated ternary mixed monolayers of phospholipid, lyso-lipid, and fatty acid [5]. In complete absence of enzyme, negatively charged, phase separated domains resembling PLA_2 domains are observed in these ternary mixed monolayers and adsorb water-solu-

* Corresponding author. E-mail: grainger@lamar.colostate.edu. Fax: +1 (303) 4911801.

SSDI 0005-2736(94)00316-5

ble cationic fluorescent dyes. Ternary mixed monolayer phase separation and dye adsorption can be blocked by lowering monolayer subphase pH, indicating that the phase separated monolayer domains comprise negatively charged fatty acids. Moreover, the presence of Ca^{2+} in alkaline monolayer subphases is essential for fatty acid phase separation [5]. This is most likely related to the ability of Ca^{2+} to chelate multiple ionized fatty acid carboxylate head groups at the monolayer interface. Further work with binary mixed monolayers of lyso-lipid and fatty acid (no enzyme present) also showed that phase separation of fatty acid regions occurred simply in response to monolayer compression. Thus, compression of binary and ternary mixed monolayers containing lipid, lyso-lipid and fatty acid results in film phase separation, leading to monolayer regions comprising fatty acid [5].

In a separate study by coworkers [6], phase separated fatty acid regions were purported to also contain lyso-lipid and/or phospholipid since PLA_2 did not adsorb to laterally phase separated, polymerized anionic diacetylenic carboxylic acid domains in a fluid phospholipid monolayer matrix. Control experiments consisting of PLA_2 injection beneath pure palmitic acid or pure C16Lyso monolayers at the air-buffer interface did not result in the formation of regular 2-D enzyme domains similar to those evidenced in dipalmitoylphosphatidylcholine (DPPC) hydrolysis experiments [3,4]. Instead, we now show that PLA_2 can electrostatically bind pure palmitic monolayers, forming a homogeneous, dense protein interfacial film having solid-like properties and lacking any resemblance to the enzyme domains. Pure lyso-lipid monolayers bind no detectable PLA_2 as determined by fluorescence microscopy.

Clearly, the presence of monolayer-resident fatty acid or lyso-lipid alone is insufficient in inducing PLA_2 domain formation that is observed during phospholipid monolayer hydrolysis. This is supported by previous work which showed that (1) enzyme domains form in partially hydrolyzed phospholipid films when substrate is still present [4] and (2) phase separated regions of regular morphology are only observed in mixed monolayers when phospholipid is

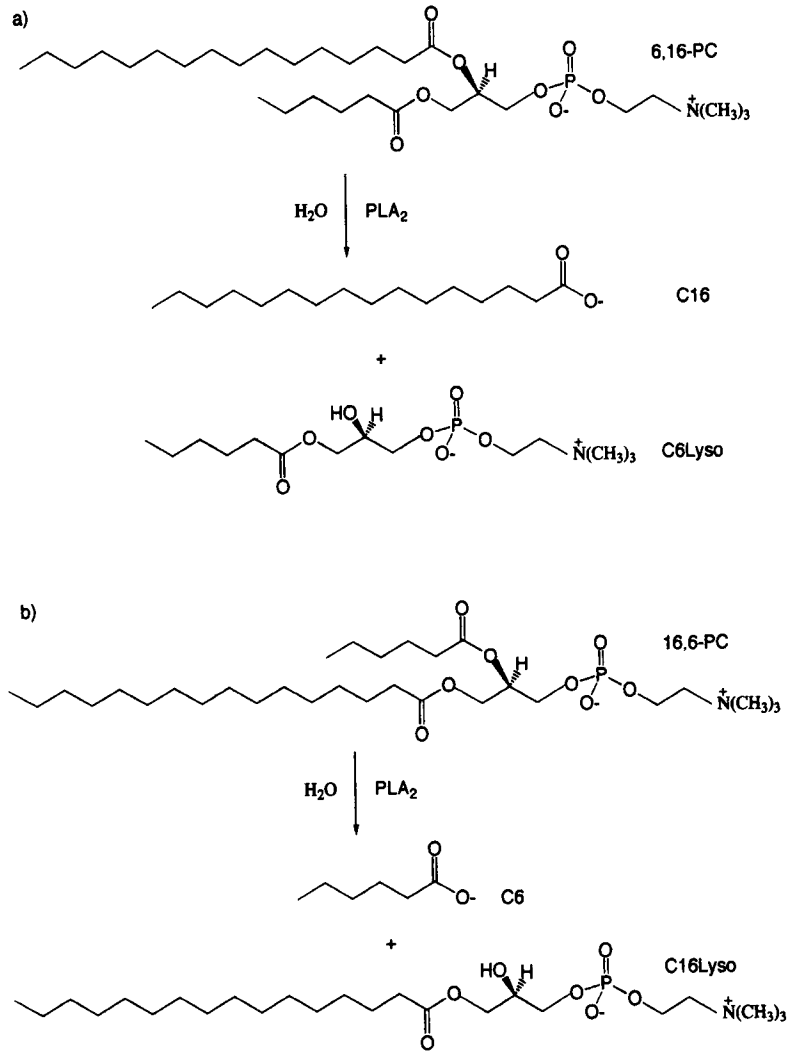

Fig. 1. Reaction products of PLA_2-catalyzed hydrolysis of (a) 6,16-PC and (b) 16,6-PC.

present. During lipid hydrolysis, membrane regions enriched in fatty acid and most likely containing small amounts of lyso-lipid and/or substrate are compelled to phase separate. While the presence of lyso-lipid and/or DPPC substrate may be important for PLA_2 interfacial binding, phase separated fatty acid reaction products are crucial for domain formation. The presence of lyso-lipid and/or phospholipid substrate together with fatty acid appears to be essential to promote phase separation into the observed regular microstructure. If phospholipid is present in phase separated monolayer regions, the stoichiometry of phospholipid to fatty acid is unknown.

According to the PLA_2-fatty acid adsorption hypothesis, enzymatic hydrolysis of asymmetric phospholipids which contain short chain, water-soluble fatty acids in the *sn*-2 position should not produce two-dimensional enzyme domains. Dissolution of fatty acid reaction products into the bulk subphase should prevent lateral monolayer phase separation of fatty acids, thus inhibiting PLA_2 domain formation. Conversely, observation of PLA_2 domains upon hydrolysis of asymmetric phospholipids containing a long chain, water-insoluble fatty acid in the *sn*-2 position and a water-soluble lyso-lipid would suggest that the presence of the corresponding lyso-lipid species is not necessary for enzyme domain formation.

We present here our investigations of PLA_2 hydrolysis of asymmetric phospholipid monolayers containing either 1-caproyl-2-palmitoyl- and 1-palmitoyl-2-caproyl-*sn*-3-phosphatidylcholine (Fig. 1) at the air/water interface. Three different enzyme sources (bovine pancreatic, bee and *N. naja naja* venom) were used in this study. Asymmetric lipid hydrolysis at the air/water interface was characterized using film balance techniques, and 'cut-off' surface pressures for PLA_2 activity were determined. Dual-label fluorescence microscopy was employed to visualize lipid monolayer-enzyme interactions in situ. In addition, measurement of surface potential and molecular area as a function of monolayer hydrolysis time allowed the characterization of the electrochemical properties of these hydrolyzed lipid monolayers.

2. Materials and methods

2.1. Materials

Bee venom and bovine pancreatic PLA_2 were purchased from Boehringer-Mannheim and Sigma, respectively, and used without further purification. *N. naja naja* venom PLA_2 was either kindly purified and supplied by Prof. M. Gelb (University of Washington) or purchased from Sigma. Both sources led to the same results. Asymmetric phospholipids 1-caproyl-2-palmitoyl-*sn*-3-phosphatidylcholine and 1-palmitoyl-2-caproyl-*sn*-3-phosphatidylcholine (Fig. 1) were synthesized by the fatty acid imidazole method using the appropriate lyso-lipid (Avanti Polar Lipids, AL) and fatty acid in a ratio of 1:5:6 lyso-lipid/fatty acid/carbonyldiimidazole (Aldrich) as described previously [7,8]. The asymmetric phospholipids were purified by elution through two silicic acid (Bio-Rad) columns with a $CHCl_3$/MeOH gradient. Analysis of the pooled PC fraction by thin layer chromatography revealed a single spot whose R_f was consistent with diacyl-PC. Isomeric purity was judged by two methods: ^{13}C-NMR spectroscopy and GC analysis after PLA_2 hydrolysis. The ^{13}C chemical shifts of α-CH_2 carbons are sensitive to chain length (especially if one is relatively short) as well as *sn*-1 versus *sn*-2 placement [8,9]. A natural abundance ^{13}C-NMR spectrum of 16,6-PC will exhibit more than 2 resonances for the α-carbon if a significant portion of 6,16-PC is also present; the detection limit by NMR is $< 10\%$. Only two α-CH_2 resonances were visible in the ^{13}C-NMR spectrum of each asymmetric lipid dissolved in CD_3OD, consistent with contamination by the other isomer of $< 10\%$. A more quantitative estimate of this value was provided by GC analysis of the fatty acids generated by PLA_2 hydrolysis of each preparation [9]. GC analysis of fatty acyl methyl esters prepared using BF_3/methanol catalysis [10] of the two separate synthetic batches of 6,16-PC yielded 2.0 and 4.4% contamination by caproic acid; for two separate batches of 16,6-PC, the contamination was 3.8 and 6.1% contamination by palmitic acid. Thus, each asymmetric PC is contaminated with the other isomer to, at most, 6%.

Rhodamine-labeled dipalmitoylphosphatidylethanolamine (DPPE-Rhod, head group-labeled, Molecular Probes, Eugene, OR), platelet activating factor (PAF, Sigma), 1-palmitoyl-2-hydroxyphosphatidylcholine (Avanti Polar Lipids) and palmitic acid (Fluka, puriss grade) were used as received. Fluorescein-conjugated phospholipase A_2 (FITC-PLA_2) was prepared as previously reported [11]. Protein concentrations were determined using the method of Smith et al. [12] and UV absorption spectra typically yielded statistical labeling efficiencies of 0.5 FITC/PLA_2. NaCl (Chempure, $> 99.9\%$), $CaCl_2$ (Chempure, $> 99.9\%$), tris(hydroxymethyl)aminomethane (Sigma, $> 99.9\%$) and bovine serum albumin (Sigma, $< 0.005\%$ fatty acid content, globulin free) were used as received. Monolayer subphases were either Millipore Nano-pure water (> 18 MΩ cm^{-1} resistivity) or NaCl/Tris/$CaCl_2$ (100:10:5; mmol) buffer with pH adjusted to 8.9 using 1.0 M HCl.

2.2. Monolayer compression isotherms

Surface pressure–area isotherms were measured with a KSV 3000 Langmuir–Blodgett film balance (KSV Instruments, Helsinki, Finland). Monolayer compression rates were 1.1 Å^2 molecule^{-1} min^{-1}. Typically, 80 μl of chloroform-dissolved lipid was spread at the air/buffer interface. To allow for solvent evaporation, monolayer

compression began 10 min after monolayers were spread. Isotherms were carried out in triplicate and were measured at 30° C.

2.3. Surface potential and surface hydrolysis measurements

Monolayer surface potential (ΔV) was measured with an ^{241}Am electrode (Nuclear Radiation Development, Grand Island, NY) positioned approx. 1–2 mm above the subphase. A platinum reference electrode was immersed in the subphase behind the compression barrier. Molecular area and surface potential were simultaneously monitored as a function of hydrolysis time at constant surface pressure using a personal computer. Lipid monolayers were spread and then compressed at 2 Å^2 molecule^{-1} min^{-1} to a surface pressure of 15 mN m^{-1}. PLA_2 (20 μg) was subsequently injected at the mouth of a milled circular Teflon mask with gentle agitation in order to allow a uniform distribution of the enzyme [3]. This mask was located beneath the surface potential electrode. The size and design of this mask were chosen to eliminate flow of the subphase outside the mask and used under conditions described by Verger for a zero-order trough [13].

2.4. Fluorescence microscopy

Fluorescence microscopy at the air/water interface was carried out on home-built mini-troughs (surface area = 9.6 cm^2 in Oregon and 50 cm^2 in Québec) mounted on stages of Zeiss ACM or Nikon epifluorescence microscopes (in Oregon and Québec, respectively). Each microscope was outfitted with optical filters to selectively excite and detect fluorescence emission of rhodamine (monolayer probe) and fluorescein (enzyme label). Monolayer compression rates were typically 2 Å^2 molecule^{-1} min^{-1}. PLA_2 was injected into the monolayer subphase (approx. 5 μg) from behind the trough barrier at 15 mN m^{-1}. When BSA was used, PLA_2 injection always followed BSA addition (30 min after BSA injection). Monolayer subphase BSA concentration was 25 nM. Fluorescence experiments were carried out at 30° C. Fluorescence images were photographed directly from the video monitor screen (in Oregon) or printed by use of a Sony video printer (in Québec).

3. Results

Surface pressure-area isotherms for 6,16-PC and 16,6-PC on buffered subphases are shown in Fig. 2. Monolayer compression isotherms for both lipids are nearly identical and exhibit only liquid-expanded behavior with no apparent phase transitions. Onsets of surface pressure occur at 175 Å^2 molecule^{-1} for both monolayers with collapse at 37 mN m^{-1} and 52 Å^2 molecule^{-1}. Pure 6,16-PC and 16,6-PC monolayers are very stable as Δarea/Δtime is

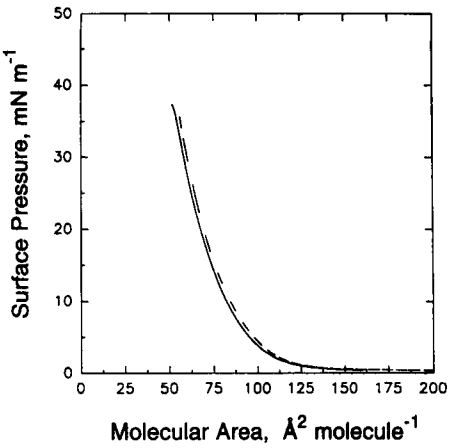

Fig. 2. Monolayer compression isotherms for 16,6-PC (—) and 6,16-PC (– – –). Compression rate is 1.1 Å^2 molecule^{-1} min^{-1}. Subphase conditions: 100 mM NaCl, 5 mM $CaCl_2$, 10 mM Tris (pH 8.9), T = 30° C.

0.02 Å^2 molecule^{-1} min^{-1} at a constant surface pressure of 30 mN m^{-1}. 16,6-PC monolayers collapse at low pressures (37 mN m^{-1}) and at a molecular area of 52 Å^2 molecule^{-1}. Comparison of 16,6-PC with DPPC monolayers at the air/water interface shows that the 10 carbon difference in the *sn*-2 acyl chain length leads to very different monolayer phase behavior. 16,6-PC does not undergo any detectable phase transitions (even at 5° C) as observed by fluorescence microscopy and surface pressure isotherms. Monolayer compression isotherms and fluorescence microscopy of DPPC show a phase transition characterized by a coexistence of solid and fluid monolayer phases [14,15]. 16,6-PC monolayers at 30° C collapse at low pressures (37 mN m^{-1}) and at a molecular area of 52 Å^2 molecule^{-1}. In contrast, DPPC monolayers are well-known to collapse at high surface pressures (70 mN m^{-1}) at 53 Å^2 molecule^{-1} at the same temperature [14]. Comparing 16,6-PC (or 6,16-PC) molecular areas at monolayer collapse with DPPC collapse areas (above critical temperature, T_c) we find that these collapse areas are similar (52 Å^2 molecule^{-1} for 16,6-PC and 6,16-PC, and 53 Å^2 molecule^{-1} for DPPC at 43° C [14]). Thus, fluid monolayer packing for 16,6-PC and 6,16-PC resembles fluid phase DPPC monolayer packing above T_c. Interestingly, interchanging the palmitic and caproic acid acyl chains in phosphatidylcholine positional isomers has little effect on observed physical monolayer properties.

N. naja naja and bee venom PLA_2 exhibit hydrolytic activity towards both 6,16-PC and 16,6-PC at all lateral surface pressures up to monolayer collapse, while pancreatic PLA_2 exhibits hydrolytic activity only at lower pressures. Decreasing monolayer surface pressures for each lipid step-wise from 30 mN m^{-1}, the upper surface pressure onset of pancreatic PLA_2 hydrolytic activity was found to be approx. 18 mN m^{-1} for both 16,6-PC and 6,16-PC (data not shown). Blocking of pancreatic PLA_2 hydrolytic activity at high monolayer surface pressures has been similarly reported using dinanoylphosphatidylcholine

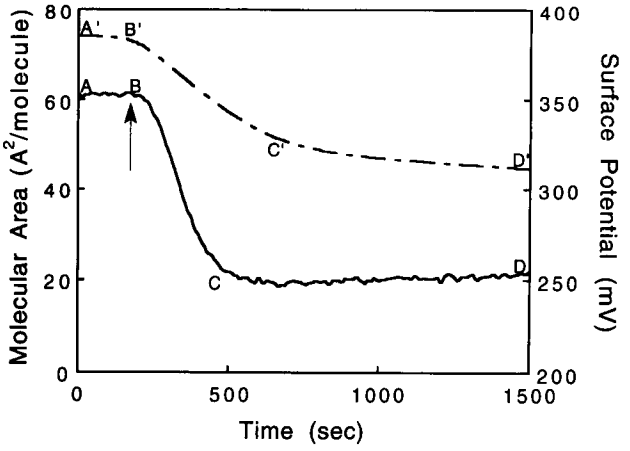

Fig. 3. Surface potential (—) and molecular area (– – –) versus 16,6-PC monolayer hydrolysis time at constant surface pressure (15 mN m^{-1}). 20 μg cobra PLA_2 injected into monolayer subphase at point B. Subphase conditions: same as in Fig 2.

substrate monolayers [16]. This previous work showed source-specific cut-offs: cobra and bee venom PLA_2 exhibited hydrolytic activity up to monolayer surface pressures of 34.8 and 35.3 mN m^{-1}, respectively, while pancreatic PLA_2-catalyzed lipid monolayer hydrolysis occurred only at much lower surface pressures (16.5 mN m^{-1}).

As shown in Figs. 3 and 4, lipid molecular area and surface potential (ΔV) at constant surface pressure (15 mN m^{-1}) are plotted as a function of hydrolysis time for *N. naja naja* PLA_2-catalyzed hydrolysis of 16,6-PC and 6,16-PC monolayers, respectively. Three distinct regions can be seen in these curves. The first segment, AB, corresponds to stable monolayer molecular area at 15 mN m^{-1} as a function of time for both pure lipid monolayers prior to the introduction of PLA_2. PLA_2 was injected into the monolayer subphase at point B (see arrow). An immediate decrease in molecular area and surface potential after enzyme injection is apparent, and continues until point C is reached. Point C corresponds exactly to the point where extrapolated segments BC and CD cross: the end of monolayer hydrolysis. Segment CD shows molecular area of the hydrolysis products remaining at the surface once hydrolysis is complete. This last segment reflects the stability of the remaining hydrolyzed mixed film.

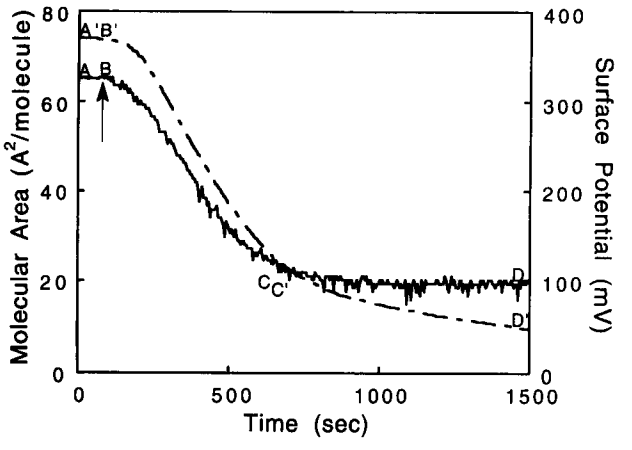

Fig. 4. Surface potential (—) and molecular area (– – –) versus 6,16-PC monolayer hydrolysis time at constant surface pressure (15 mN m^{-1}). 20 μg cobra PLA_2 injected into monolayer subphase at point B. Subphase conditions: same as in Fig. 2.

Upon completion of 16,6-PC monolayer hydrolysis (Fig. 3, point C′), short chain caproic acid reaction products (Fig. 1) should be solubilized in the monolayer subphase, with monopalmitoyl-PC (C16Lyso) remaining at the air-buffer interface. Molecular area at the end of 16,6-PC hydrolysis should thus correspond to the area of a pure C16Lyso monolayer at this surface pressure (50 $Å^2$ $molecule^{-1}$). Fig. 3 shows that molecular area for PLA_2-hydrolyzed 16,6-PC monolayers decreases from 74 to 49.5 $Å^2$ $molecule^{-1}$ (from point B′ to C′), almost identical to the area of a pure C16Lyso monolayer under these conditions. Slow decreases in molecular area subsequently observed in segment C′D′ from 49.5 to 45 $Å^2$ $molecule^{-1}$ are due to the intrinsic instability of the residual C16Lyso monolayer. Indeed, pure C16Lyso monolayers compressed to 15 mN m^{-1} show time-dependent molecular areas which slowly decrease with a slope very similar to the slope of segment C′D′ (data not shown).

Similarly, in Fig. 3 the observed decrease in surface potential from 357 to 248 mV (from point B to C) upon PLA_2 hydrolysis is due to the change in the electrochemical properties of the film. The surface potential for pure 16,6-PC monolayers before PLA_2 hydrolysis (point B, 357 mV) decreases to a value (point C, 248 mV) close to the surface potential for pure C16Lyso monolayers (220 mV, data not shown) under the same conditions. In contrast to molecular area data, the slope of segment CD remains nearly zero once PLA_2 hydrolysis is complete with only a small observable increase in surface potential (248 to 257 mV) over time. For this experiment, we have estimated that the 6% 6,16-PC impurity can lead to a difference of approx. 10 mV in the final value for the surface potential and approx. 3 $Å^2$ $molecule^{-1}$ in the final molecular area. It is thus clear that such a small difference does not affect our results.

Similar behavior can be seen in Fig. 4 for *N. naja naja* PLA_2-catalyzed hydrolysis of 6,16-PC monolayers. However, in this case, palmitic acid reaction products remain at the interface and the monocaproyl-PC (C6Lyso) product is solubilized in the monolayer subphase (Fig. 1). Dissolution of C6Lyso leads to very large decreases in molecular area (from 74 to 19 $Å^2$ $molecule^{-1}$, segment B′C′) and in surface potential (from 328 to 100 mV, segment BC). Monolayer molecular area at point C′ very closely matches the area for pure palmitic acid monolayers under these conditions (19.4 $Å^2$ $molecule^{-1}$ [5,17]). However, the surface potential at point C (100 mV) is much larger than that for pure palmitic acid monolayer under similar conditions (−30 mV, data not shown). We have estimated that

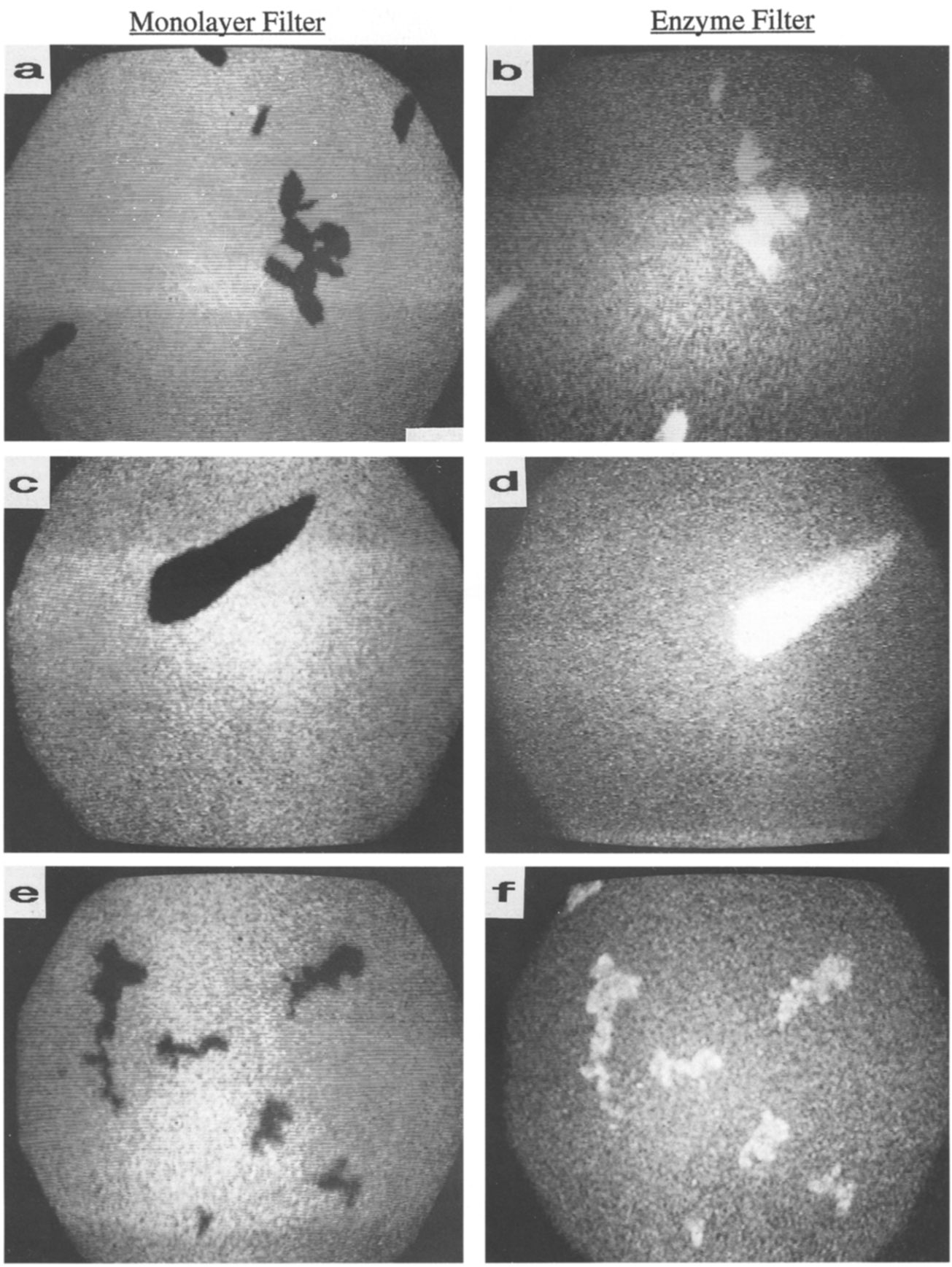
Monolayer Filter
Enzyme Filter
a
b
c
d
e
f

the 4% 16,6-PC impurity leads to a difference of approx. 5 mV in the final surface potential measurements and 1 square angstrom per molecule in the final film molecular area. These small differences can also be neglected and do not affect our results. A flat plateau in surface potential is observed when lipid hydrolysis is complete (segment CD), whereas a steady decrease in molecular area is observed from point C′ to D′. This decrease in molecular area is due to the intrinsic instability of pure palmitic acid monolayers under these conditions. Pure palmitic acid films compressed to 15 mN m^{-1} show molecular areas which decrease slowly over time. This rate of change in molecular area is similar to that seen in the slope of segment C′D′. Use of bee or pancreatic PLA_2 produces surface potential and molecular area kinetics similar to that shown in Figs. 3 and 4 for the cobra PLA_2.

PLA_2 action on 6,16-PC and 16,6-PC monolayers was further characterized using dual-label fluorescence microscopy at the air/water interface. Fig. 5 shows fluorescence micrographs of PLA_2-hydrolyzed 6,16-PC monolayers after 90 min. Image pair 5a and b correspond to *N. naja naja* PLA_2-hydrolyzed monolayers while c and d, and e and f correspond to bee venom and bovine pancreatic PLA_2-hydrolyzed monolayers, respectively. Figs. 5a, c, and e are imaged through a rhodamine-specific filter, revealing the location of lipid monolayer (Rhod-DPPE) probe approx. 90 min after enzyme injection. Phase separated gray regions surrounded by brighter fluid phase lipid are evident. These domains appear gray due to selective partitioning and enrichment of the rhodamine-labeled lipid probe into the surrounding fluid monolayer phase [15,18]. Figs. 5b, d, and f are imaged with a fluorescein-specific filter and show the location of fluorescein-labeled PLA_2 [3,4]. The location of FITC-PLA_2 consistently corresponds to the phase separated gray regions shown in micrographs 5a, c, and e, supporting adsorption of PLA_2 specifically to these areas.

In contrast, several hours are necessary to observe any PLA_2 domain formation upon hydrolysis of fatty acid-soluble 16,6-PC lipid monolayers. PLA_2 domains that are observed after long waiting periods are smaller and fewer in number than PLA_2 domains observed with fatty acid-insoluble 6,16-PC monolayer hydrolysis (Fig. 6). They also lack any appreciable regular morphology. Moreover, addition of fatty acid-binding bovine serum albumin (BSA) to the 16,6-PC monolayer subphase results in total suppression of PLA_2 domain formation. Several control experiments were conducted to assess the possibility that lipid impurities in 16,6-PC monolayers might be responsible for the observed PLA_2 domain formation. In particular, lipid positional isomers as by-products of the synthesis and acyl chain migration products could contribute to the presence of 6,16-PC contaminants in otherwise pure 16,6-PC samples. As described in the experimental section, 16,6-PC lipid samples contained between 3.8 and 6.1% 6,16-PC. Given this level of impurity in the 16,6-PC lipid sample, a completely hydrolyzed 16,6-PC monolayer should consist of 94% C16Lyso (from 16,6-PC) and 6% palmitic acid (from the 6,16-PC impurity). The caproic acid and C6Lyso reaction products from 16,6-PC and 6,16-PC, respectively, are solubilized. Therefore, a binary mixed monolayer consisting of 94% C16Lyso and 6% palmitic acid would be expected from this experiment in the worst case. To test this scenario for possible influence on PLA_2 domain formation, a monolayer of 94% C16Lyso and 6% palmitic acid was compressed to 15 mN m^{-1} and imaged using fluorescence microscopy. Results showed that at 15 mN m^{-1}, the monolayer remained completely fluid, showing no evidence of palmitic acid phase separation within the microscope's resolution. Moreover, compression of this binary mixed monolayer to 15 mN m^{-1} followed by injection of FITC-labeled PLA_2 into the subphase lead to no observable enzyme domain formation even after a 10 h incubation period. Based on the enzyme domain data presented in Fig. 6, and the results of the preceding control experiments, PLA_2 domain formation in the 16,6-PC case does not appear to be due to the 6% 6,16-PC impurity found in 16,6-PC lipid samples.

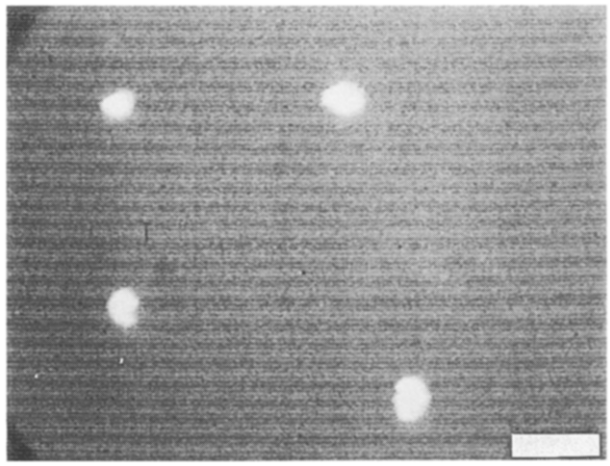

Fig. 6. Fluorescence micrograph of cobra PLA_2 hydrolyzed 16,6-PC monolayers as viewed through a fluorescein filter. Same experimental conditions as in Fig. 2. Scale bar = 50 μm.

Fig. 5. Fluorescence micrographs of PLA_2 hydrolyzed 6,16-PC monolayers 90 min after enzyme injection. Micrographs in a, c, and e were imaged through a rhodamine-specific fluorescence filter whereas b, d, and f were imaged through a fluorescein-specific fluorescence filter. Phase separated regions observable in a, c and e correspond exactly to the location of FITC-labeled PLA_2 fluorescence in b, d and f. Image pairs a–b, c–d and e–f correspond to cobra, bee and pancreatic PLA_2 hydrolyzed monolayers, respectively. Monolayer hydrolysis was carried out at constant surface pressure (15 mN m^{-1}). Subphase conditions: same as in Fig. 2. Scale bar in a is 25 μm.

Addition of BSA to 6,16-PC monolayer subphases during PLA_2-catalyzed hydrolysis does not have any effect upon PLA_2 domain formation. Additionally, identical hydrolysis experiments performed with PLA_2 using platelet activating factor (PAF, 1-*O*-alkyl-2-acetyl-*sn*-3-phosphatidylcholine) result in the formation of water-soluble acetic acid and a long-chain surface active lyso-lipid were compared with the behavior of 16,6-PC. PLA_2 hydrolysis of PAF monolayers failed to produce PLA_2 domains at the air/buffer interface as evidenced by fluorescence microscopy (data not shown). Significantly, pure monolayers of palmitic acid and lyso-lipid were each exposed to fluorescent-labeled PLA_2. Both experiments failed to produce monolayer domains resembling that from other hydrolysis experiments. While lyso-lipid monolayer experiments were identical to PAF results (i.e., no observable enzyme binding), pure palmitic acid monolayers promoted homogeneous adsorption of enzyme to the interface, producing condensed protein films shown in Fig. 7a. These adsorbed PLA_2 films do no exhibit any microstructure except where regions of the PLA_2-palmitic acid film are devoid of protein (no fluorescence). Regions devoid of PLA_2 appear to be due to the protein-fatty acid film cracking in response to uncontrolled monolayer surface flow. Moreover, upon monolayer expansion after adsorption at a lateral pressure of 15 mN m^{-1}, additional defect sites are apparent, suggesting the protein fatty acid composite film fractures even further (Fig. 7b). Indicative of a solid-state film, this property is inconsistent with results from previous enzyme domain formation in other monolayer systems where PLA_2 domains were not observed to undergo deformation or fracture at high or low surface pressures [3–6].

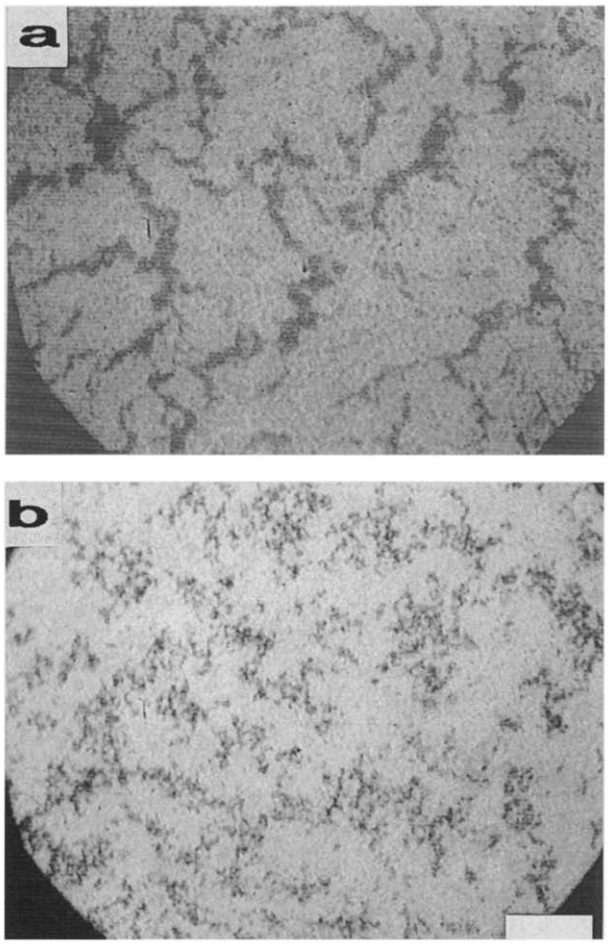

Fig. 7. Fluorescence micrographs of fluorescein-labeled PLA_2 adsorbed to monolayers of pure palmitic acid (a) after enzyme injection at constant lateral surface pressure of 15 mN m^{-1}. (b) Same monolayer decompressed to lateral surface pressure of 0 mN m^{-1}, showing solidified film fracture involving both protein and fatty acid. No regular enzyme microstructures are observed. No lipid fluorescent probe is present: signal is only associated with membrane localized PLA_2. Scale bar = 50 μm (same as Fig. 6). Subphase same as in Fig. 2.

4. Discussion

We and coworkers have previously proposed that, under suitable conditions, critical amounts of PLA_2-produced fatty acids lead to hydrolyzed monolayer lateral phase separation of negatively charged fatty acids [3,4]. Positively charged PLA_2 amino acid residues, known from the three-dimensional crystal structures of these enzymes to form surface-exposed cationic patches [19–21], then bind electrostatically to negatively charged fatty acid microstructures. PLA_2 hydrolysis studies using isomeric asymmetric phospholipid monolayers that produce water-soluble fatty acid products in one case and water-soluble lyso-lipid in another (Fig. 1) have been used in this work to help elucidate the mechanism of enzyme domain formation.

The central tenet of the enzyme domain formation hypothesis is that PLA_2-produced fatty acid reaction products laterally phase separate after hydrolysis, with electrostatically driven enzyme adsorption either concomitant with or subsequent to this monolayer microstructuring [3,4]. Consequently, if fatty acid reaction products are removed from the monolayer interface, PLA_2 adsorption would be inhibited. This is accomplished using enzyme-produced water-soluble fatty acid reaction products such as the 16,6-PC substrate (Fig. 1).

Surface potential and molecular area data after hydrolysis of 16,6-PC (Fig. 3) closely correspond to that of pure C16Lyso. This directly supports rapid solubilization of short-chain caproic acid products into the subphase during hydrolysis. However, fluorescence microscopy does not entirely support this conclusion. Small PLA_2 domains are still observed with microscopy after long periods of incubation (Fig. 6). If the hypothesis is correct, caproic fatty acids should be associated with these PLA_2 domains at the interface. These results could be explained by the well known interactions between PLA_2 and solubilized fatty acids [22] which would occur in the bulk subphase, pro-

moting delayed enzyme adsorption to the interface. PLA_2 interaction with soluble caproic acid in the subphase by an acylation mechanism or simply ion-pair formation with basic amino acids [22] would render the enzyme more surface active and promote interfacial domain formation.

Although the precise mechanism remains unelucidated, the involvement of caproic acid in the formation of these small PLA_2 domains has been clearly demonstrated by removing surface-bound or water-solubilized fatty acids with the BSA-fatty acid binding protein.

In addition to PLA_2-fatty acid interactions, the affinity of bovine serum albumin to solubilized fatty acid species is also well documented [23]. PLA_2 hydrolysis of 16,6-PC monolayers with BSA in the monolayer subphase yields no observable interfacial enzyme aggregation (even after long incubation periods). Addition of BSA thus completely prevents formation of PLA_2 domains. In accord with our adsorption hypothesis [4–6], enzyme-produced water-soluble fatty acid apparently leaves the interface, thereby preventing monolayer fatty acid interfacial aggregation, the critical step for PLA_2 domain formation.

In PLA_2-hydrolyzed 6,16-PC monolayer systems, reaction products are the water-soluble monocaproyl-PC (C6Lyso) and the water-insoluble palmitic acid (Fig. 1). Since palmitic acid remains in the monolayer after hydrolysis, positively charged PLA_2 surface residues are able to interact electrostatically with anionic fatty acid carboxylate head groups resident at the interface, forming 2-D domains as evidenced by fluorescence microscopy (see Fig. 5). Results in Fig. 4 show that monolayer molecular area reaches that expected for palmitic acid (point C) after hydrolysis, suggesting that it is the only product remaining at the interface. However, the surface potential at the end of the hydrolysis (point C, 100 mV, Fig. 4) does not correspond to that for pure palmitic acid at this surface pressure (−30 mV).

For net neutral monolayers like phosphatidylcholine and lysophosphatidylcholine, the surface potential depends mainly on the vertical component of the resultant dipole moment of the molecules present at the interface. Thus, net neutral compounds, 16,6-PC, 6,16-PC and lyso-lipid, contribute the following dipole moments to the observed surface potential: the terminal methyl at the end of each fatty acid chain, the carbonyl group (one for each fatty acid), the ester bond between each fatty acid and the glycerol backbone, the dipole between the negative charge on the phosphate moiety and the positive charge on the choline quaternary nitrogen (see Fig. 1) as well as oriented interfacial water molecules [24].

Once the hydrolysis of 6,16-PC is completed (point C, Fig. 4), only the fatty acid hydrolysis product should contribute to the observed surface potential: all lyso-lipid species should be solubilized into the subphase (as evidenced by the observed molecular area). Monolayer-resident palmitic acid bears a net negative charge on the carboxyl residue (Fig. 1) at the experimental pH (8.9). Thus, in this case, in addition to the contribution from the vertical dipole moment, the surface potential also results from the presence of an ionized monolayer (negative charge) which leads to a potential difference between the surface and the bulk of the pure subphase [25]. The observed large decrease in surface potential after PLA_2 film hydrolysis is due to the removal of dipole moments contributed by lyso-lipid species and the formation of a new ionized species (palmitic acid). However, a large difference exists between the observed final value of surface potential (100 mV) and that expected (−30 mV) for a film of pure palmitic acid. The only apparent explanation is the contribution of adsorbed PLA_2 to the surface potential. As observed in Fig. 5, PLA_2 forms numerous, large, two-dimensional domains after 6,16-PC hydrolysis. Any charge or dipolar contribution from surface-bound PLA_2 will continuously change the surface potential during the course of formation of these PLA_2 domains. When considering the size of these domains (see Fig. 5) and the number of charges and dipoles present in this enzyme (e.g., p*I* of *N. naja naja* PLA_2 is 4.95 [26]), this large difference (130 mV) between the surface potential at the end of the hydrolysis and that for pure palmitic acid is not surprising. This result also strongly suggests that bound PLA_2 does not change the molecular area (or surface pressure) of the fatty acid monolayer. PLA_2 in these domains thus does not significantly protrude into the fatty acid monolayer, contrary to what is observed when a phospholipid monolayer is present. In this case, enzyme-substrate recognition and binding occurs and, in order to hydrolyze the phospholipid monolayer, PLA_2 must at least partially penetrate into the substrate monolayer. The result is the frequent observation of small increases (< 5 mN m^{-1}) in surface pressure at hydrolytic onset. In the present case, the data suggest that PLA_2 does not protrude into the fatty acid monolayer because it does not change the final molecular area. Nevertheless, the surface potential properties of the film are drastically affected by its presence. It is thus proposed that the interfacial binding of PLA_2 onto final palmitic acid films involves electrostatic interactions. This is supported by results of PLA_2 adsorption to pure palmitic acid films (Fig. 7) where homogeneous and uniform PLA_2 adsorption actually solidifies the film by electrostatic interactions.

BSA experiments were also performed with 6,16-PC monolayers to determine if BSA was able to remove or block monolayer resident palmitic acid reaction products. Results of these experiments with *N. naja naja*, bee venom, and pancreatic hydrolyzed monolayers are all almost identical to those of Fig. 5, showing identical locations for phase separated gray monolayer regions and FITC-labeled PLA_2. Apparently, BSA cannot bind or remove surface-resident, largely water-insoluble palmitic acid reaction products. This result is consistent with previous investigations showing BSA is unable to bind interfacial long-chain fatty acids [27]. Furthermore, BSA is unable to

remove palmitic acid from the interface and, therefore, is not effective in inhibiting formation of PLA_2 domains.

The goal of our research is to elucidate the mechanism of PLA_2 domain formation in hydrolyzed lipid monolayers. The data presented here show that release of PLA_2-produced water-soluble fatty acid reaction products from 16,6-PC into the subphase inhibits enzyme domain formation, indicating monolayer-bound fatty acids play an essential role in both the monolayer phase separation and the enzyme binding events.

Our and coworkers' previous work [5,6], demonstrated with DPPC/C16Lyso/palmitic acid (0.2:1:1; mol/mol) ternary mixed monolayers that lateral phase separation was observed at basic pH in the presence of calcium even in the absence of PLA_2, yielding monolayer lipid domain morphologies that are similar to PLA_2 microstructures yet without enzyme. The DPPC/C16lyso/palmitic acid ternary mixed monolayers used in these phase-separation studies represented monolayer compositions present at different extents of enzyme hydrolysis (PLA_2 was absent, yet phase separation still occurs). In addition, we observed binding of cationic water-soluble carbocyanine dyes to the phase separated domains in DPPC/C16Lyso/palmitic acid (0.2:1:1) ternary mixed monolayer systems [5], showing that phase-separated domains in the monolayer are negatively charged (fatty acid enriched). We also showed that phase separation of negatively charged domains in DPPC/C16Lyso/palmitic acid ternary mixed monolayers could be readily blocked by removing Ca^{2+} from the subphase, as evidenced by fluorescence microscopy [5]. Since divalent cations are well known to induce lateral phase separation in negatively charged monolayers at the air/water interface [28], this further supports our contention. Furthermore, reducing the pH of DPPC/C16Lyso/palmitic acid (0.2:1:1) monolayer subphases (with Ca^{2+} present in subphase) did not inhibit phase separation [5], but we were unable to observe cationic dye binding to these monolayer domains. Thus, electrostatic interactions in heterogeneous ternary mixed monolayers comprising diacylphosphatidylcholines (PLA_2 substrates), lyso-lipid and fatty acid reaction products are essential determinants of monolayer phase behavior. These previous results and those presented in this paper support the conclusion that PLA_2-produced fatty acids play a crucial role in controlling both subsequent enzyme interfacial response and the formation of enzyme domains.

Compared to results reported by Reichert and coworkers [6], work presented here extends and complements what is known about these monolayer systems. Phase separation in model ternary mixed or PLA_2-hydrolyzed monolayers leading to dye or enzyme binding only occurs in the presence of both membrane-resident phosphatidylcholine and fatty acid. Fluorescence microscopy of phase separated ternary mixed monolayers reveals that these regions are gray [5,6], not black, indicating that small amounts of monolayer fluorescent lipid probe are present in phase separated regions. This suggests these regions are not highly condensed. If fluorescent-labeled lipid probe is present in these regions, it is not surprising that unlabeled phospholipid may also be present. This is consistent with results from Reichert and coworkers that showed PLA_2 would not bind to phase separated, condensed diacetylenic fatty acid regions within a fluid D-DPPC matrix [6]. These observations support the contention that, during ternary mixed monolayer compression [5,6] or PLA_2-mediated monolayer hydrolysis [3,4], phospholipid substrate becomes entrapped in monolayer regions enriched in fatty acid. This is also consistent with the observation that PLA_2 forms domains in hydrolyzed monolayer systems before phospholipid hydrolysis is complete. Electrostatically driven PLA_2-membrane interactions coupled with specific PLA_2-substrate binding appear necessary to form regular phase separated enzyme domains.

The shapes of PLA_2 domains in hydrolyzed DPPC and 6,16-PC systems are dissimilar. As previously reported, bean-shaped enzyme domains form in response to enantiomerically pure DPPC monolayer hydrolysis [3,4]. Bean-shaped microstructures are also observed during compression of ternary mixed monolayers containing enantiomerically pure DPPC, C16Lyso and palmitic acid (0.2:1:1) [5]. Significantly, DPPC is well known to exhibit chiral lipid domains at the air/water interface in the phase transition region [15,18,29,30]. DPPC chiral lipid domains may also play a role in orchestrating PLA_2 interfacial self-assembly. This property may also apply to chiral C16Lyso even though it lacks a phase transition and does not form monolayer domains on the microscopic scale [5]. Hydrolysis of 6,16-PC monolayers results in irregularly shaped PLA_2 domain formation (Fig. 5). Obtaining regular, bean-shaped PLA_2 domains observed during DPPC hydrolysis may depend on the presence of DPPC and/or lyso-lipid trapped in fatty acid enriched membrane regions. In 6,16-PC systems, lyso-lipid reaction products are solubilized during hydrolysis resulting in conversion to a pure fatty acid monolayer. In this case, PLA_2 interfacially self-assembles, but enzyme domains are not bean-shaped (Fig. 5). That is, PLA_2 interfacially adsorbs to fatty acid without the morphology imposed by chiral lipids present at the interface. Control experiments showing PLA_2 adsorption to pure palmitic acid monolayers support this contention (Fig. 7). We therefore alter our original PLA_2 domain formation hypothesis to include some level of chiral phospholipid within fatty acid-enriched membrane regions. Chiral phospholipid is hypothesized to control resulting enzyme domain morphology by structuring the interfacial film onto which PLA_2 binds. Future work is aimed at determining the chemical composition of phase separated monolayer domains.

In conclusion, asymmetric 6,16-PC and 16,6-PC lipids have been shown to be valuable model compounds to test our hypothesis concerning PLA_2 binding to heterogeneous model monolayer membranes. The capability to selectively

produce water-soluble or water-insoluble PLA_2 hydrolysis products in lipid monolayers has allowed us to further describe the role of fatty acids and lyso-lipids on influencing PLA_2 interaction with lipid monolayer membranes. Furthermore, these data have allowed direct correlation of the presence of insoluble, monolayer-localized fatty acids with binding of PLA_2 from the subphase and formation of laterally phase separated monolayer microstructures of both lipids and enzyme.

Acknowledgements

We thank Professor M. Gelb, University of Washington, for supplying purified *N. naja naja* PLA_2. Financial support from National Science Foundation grant DMR-9357439 (D.W.G.), Natural Sciences and Engineering Research Council of Canada, The Fonds FCAR, and the FRSQ (C.S.), NATO Travel Grant (D.W.G. and C.S.), and National Institutes of Health grant GM26762 (M.F.R.) is greatly appreciated. A scholarship from the Fonds FCAR (M.G.) is also acknowledged.

References

[1] Dennis, E.A. (1983) in The Enzymes, 3rd Edn. (Boyer, P.D., ed.), Vol. 16, pp. 307–353, Academic Press, New York.
[2] Pieterson, W.A., Vidal, J.C., Volwerk, J.J. and deHaas, G.H. (1974) Biochemistry 13, 1455–1460.
[3] Grainger, D.W., Reichert, A., Ringsdorf, H. and Salesse, C. (1989) FEBS Lett. 252, 79–85.
[4] Grainger, D.W., Reichert, A., Ringsdorf, H. and Salesse, C. (1990) Biochim. Biophys. Acta 1023, 365–379.
[5] Maloney, K.M. and Grainger, D.W. (1993) Chem. Phys. Lipids 65, 31–42.
[6] Reichert, A., Ringsdorf, H. and Wagenknecht, A. (1992) Biochim. Biophys. Acta 1106, 178–188.
[7] Burns, R.A., Donovan, J.M. and Roberts, M.F. (1983) Biochemistry 22, 964–973.
[8] Burns, R.A. and Roberts, M.F. (1980) Biochemistry 19, 3100–3106.
[9] Lewis, K.A., Bian, J. and Roberts, M.F. (1990) Biochemistry 29, 9962–9970.
[10] Metcalfe, L.D. and Schmitz, A.A. (1961) Anal. Chem. 33, 363–364.
[11] Nargessi, R.D. and Smith, D.S. (1986) Methods Enzymol. 122, 67–73.
[12] Smith, P.K., Krohn, R.I., Hermanson, G.T., Mallia, A.K., Gartner, F.H., Provenzano, M.D., Fujimoto, E.K., Goeke, N.M., Olson, B.J. and Klenk, D.C. (1985) Anal. Biochem. 150, 76–85.
[13] Verger, R. and deHaas, G.H. (1973) Chem. Phys. Lipids 10, 127–136.
[14] Albrecht, O., Gruler, H. and Sackmann, E. (1978) J. Phys. (Paris) 39, 301–313.
[15] McConnell, H.M., Tamm, L.K. and Weis, R.M. (1984) Proc. Natl. Acad. Sci. USA 81, 3249–3253.
[16] Demel, R.A., Geurts van Kessel, W.S.M., Zwall, R.F.A., Roelofsen, B. and Van Deenen, L.L.M. (1975) Biochim. Biophys. Acta. 406, 97–107.
[17] Albrecht, O. (1989) Thin Solid Films 178, 93–101.
[18] Peters, R. and Beck, K. (1983) Proc. Natl. Acad. Sci. USA 81, 3249–3253.
[19] Dijkstra, B.W., Kolk, K.H., Hol, W.G.J. and Drenth, J. (1981) J. Mol. Biol. 147, 97–123.
[20] Scott, D.L., Otwinowski, Z., Gelb, M.H. and Sigler, P.B. (1990) Science 250, 1563–1566.
[21] White, S.P., Scott, D.L., Otwinowski, Z., Gelb, M.H. and Sigler, P.B. (1990) Science 250, 1560–1563.
[22] Cho, W., Tomasselli, A.G., Heinrikson, R.L. and Kezdy, F.J. (1988) J. Biol. Chem. 263, 11237–11241.
[23] Lehninger, A.L. (1982) Principles of Biochemistry, p. 702, Worth Publishers, New York.
[24] Vogel, V. and Mobius, D. (1988) J. Colloid Interface Sci. 126, 408–420.
[25] Gaines, G. L., Jr. (1966) Insoluble Monolayers at Liquid-Gas Interfaces, pp. 191–195, John Wiley, New York.
[26] Waite, M. (1978) The Phospholipases (Handbook of Lipid Research, Vol. 5), p. 167, Plenum Press, New York.
[27] Kupferberg, J.P., Yokoyama, S. and Kezdy, F.J. (1981) J. Biol. Chem. 256, 6274–6281.
[28] Eklund, K.K., Vuorinen, J., Mikkola, J., Virtanen, J.A. and Kinnunen, P.K.J. (1988) Biochemistry 27, 3433–3437.
[29] Meller, P. (1988) Rev. Sci. Instrum. 59, 2225–2231.
[30] Losche, M., Sackmann, E. and Mohwald, H. (1983) Ber. Bunsenges. Phys. Chem. 87, 848–852.